Porosity Characterization of Activated Carbons From Wood Precursors *via* Small Angle Neutron Scattering

J. M. Calo,* F. S. Baker,† and P. J. Hall‡
*Division of Engineering, Brown University, Providence, RI 02912
†Oak Ridge National Laboratory, Oak Ridge, TN 37831-6087
‡Department of Chemical Engineering, Strathclyde University, Glasgow, Scotland, UK

Introduction

Activated carbon products are used in a wide range of commercial gas and liquid phase applications, ranging from control of gasoline emissions from vehicles to purification of drinking water through "end-of-tap" filters. Commercial activated carbon products are produced from organic materials that are rich in carbon; notably coal, lignite, wood, nut shells, peat, pitches, and cokes [1]. Manufacturing processes fall into two categories - thermal activation and chemical activation. The effective porosity of activated carbon produced by thermal activation is the result of gasification of the carbon at relatively high temperatures [2], but the porosity of chemically-activated products is generally created by chemical dehydration reactions occurring at significantly lower temperatures [3].The vast majority of applications exploit the highly developed and accessible internal pore structure of activated carbon materials [1]. An understanding of what pore structure characteristics are required for a given application and how they can be produced is of paramount importance in developing a viable activated carbon product for the application. In helping to achieve this objective, one must have on hand techniques for characterizing the pore structure and surface area of an activated carbon material. Traditionally, gas adsorption techniques have been used for this purpose, but these alone generate only a partial, albeit important picture of the nature of the pore structure in an adsorbent. To complement gas adsorption data, more direct techniques of characterizing pore structure have been applied in recent years, including high resolution transmission electron microscopy (HRTEM), small angle X-ray scattering (SAXS) and small angle neutron scattering (SANS). This paper focuses on gas adsorption and SANS data obtained on chemically-activated, wood-based carbons of different pore structures and pore size distributions.

Experimental

Activated Carbon Samples. Activated carbon Samples 1-3 were produced by the chemical activation of wood with phosphoric acid, a process that is used commercially for the production of highly porous, high surface area products [1]. In addition, the activated carbon products represented by Samples 1 and 3 were obtained by subjecting a conventional phosphoric acid-activated carbon product to a second stage of activation with an alkali; in this instance, potassium hydroxide. It has been demonstrated that a second stage of alkali activation is highly beneficial in manipulating the porosity of activated carbon over a very wide range, not only with respect to pore width, *per se*, but also to the "tightness" of the size distribution [4,5]. An additional and probably unique

benefit of the second stage of alkali activation is that the carbons so obtained are exceptionally pure, certainly by typical commercial product standards, exhibiting very low inorganic matter content of <0.1% by weight. Thus, alkali-activated carbons represent good model activated carbon materials for fundamental studies, such as discussed here. Whereas the alkali activation conditions for the preparation of Sample 1 were selected for production of a highly microporous product with a narrow pore size distribution, those for Sample 3 were designed to yield a product with a similar micropore volume (i.e., in pore widths of < 2 nm) but also a relatively large volume of mesopores (i.e., in pore widths of 2-50 nm). Some of the process variables that are influential in this respect are discussed elsewhere [4, 6-8]. Sample 4, although not an activated carbon product in the commercial sense, was included in the study as an example of a high surface area, highly mesoporous carbon material that also exhibits a relatively low inorganic content. It was a commercial carbon black product, "Black Pearls 2000," produced by the Cabot Corporation.

The four carbon samples were characterized using well-established gas adsorption techniques. Nitrogen adsorption isotherms were determined on a Micromeritics instrument at 77 K. Surface areas obtained from the isotherm data by application of the Brunauer-Emmett-Teller (BET) theory [9]. Pore size distributions were determined using the Barrett-Joyner-Halendar (BJH) [10] and density functional theory (DFT) [11, 12] methods. The gas adsorption data are summarized in Table I.

Neutron Scattering. The small angle neutron scattering (SANS) data were obtained at the Intense Pulsed Neutron Source (IPNS) of the Argonne National Laboratory on the time-of-flight Small-Angle Neutron Diffractometer (SAND). This instrument has a 40 x 40 cm^2 area detector with a wavevector range $0.035 < Q < 6$ nm^{-1}. The sample holders were made of Suprasil with a pathlength of 0.1 cm. The scattering data were corrected for scattering from the sample holder and other instrumental backgrounds. Normalization for the sample thickness and transmission was made, and the data were scaled to yield absolute calibrations. The neutron scattering density of carbon is 5.6×10^{10} cm^{-2}, which is very close to that of perdeuterated toluene that was used for contrast matching in the current experiments. Essentially, granulated char samples were mixed with perdeuterated toluene and allowed to come to equilibrium by immersion in an ultrasonic bath for a minimum of 4h.

Results and Discussion

In Figure 1 are presented cumulative pore size distributions (PSD) of the carbon samples obtained from DFT analysis of nitrogen adsorption isotherms at 77K. The data for the smaller porosity only, were reasonably well fit with Schulz (gamma-type) distribution functions (solid curves).

$$f(R,R_0,b) = \frac{1}{\Gamma(b)}\left(\frac{b}{R_0}\right)^b R^{(b-1)} e^{-(bR/R_0)} \qquad [1]$$

where R is the pore radius, and R_0 and b are constants. The resultant parameter values are listed in the caption of Figure 1.

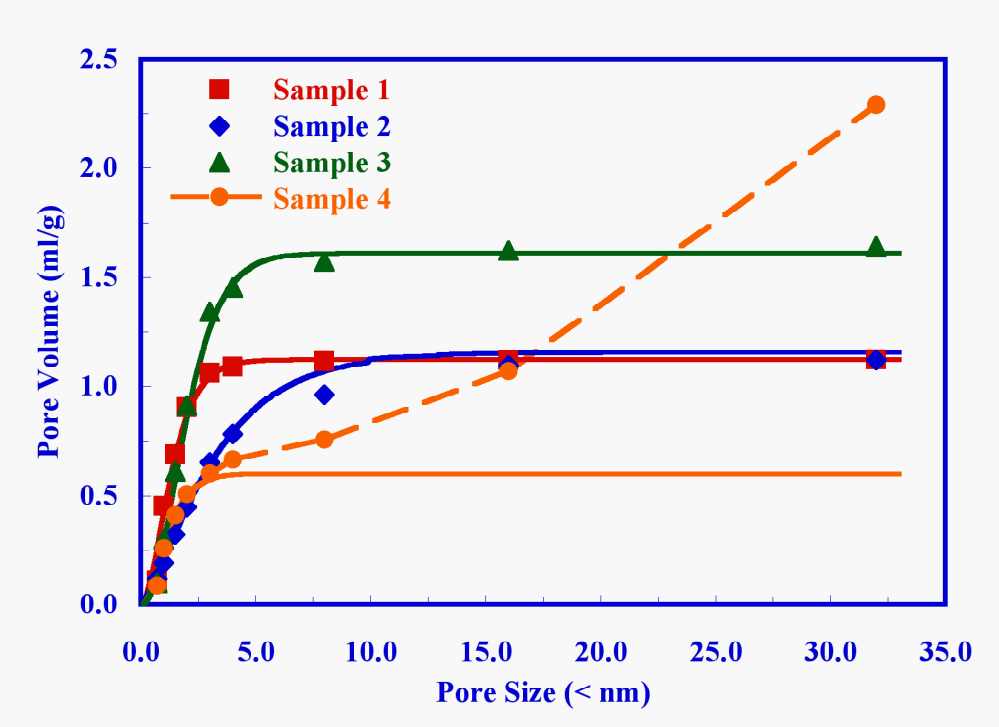

Figure 1. Integral pore size distributions of the activated carbon samples obtained from DFT analysis of nitrogen adsorption isotherms at 77K. The solid curves are cumulative (integral) Schulz distribution fits of the small porosity data only. Schulz distribution parameter values Sample#(R_0,b): 1(0.75,2.5); 2(1.7,1.5); 3(1.1,3.0); 4(0.7,3.0); for R in nm.

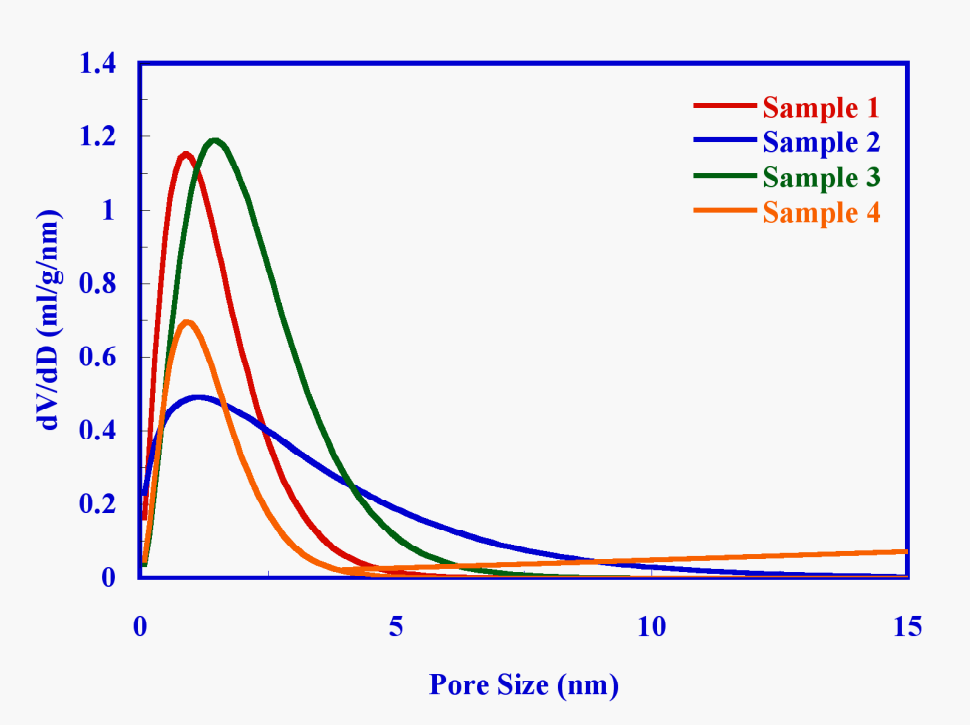

Figure 2. Differential pore size distributions of the activated carbon samples obtained from differentiation of the Schulz distribution function fits to the data in Figure 1, and also the derivative of the larger porosity data for Sample 4.

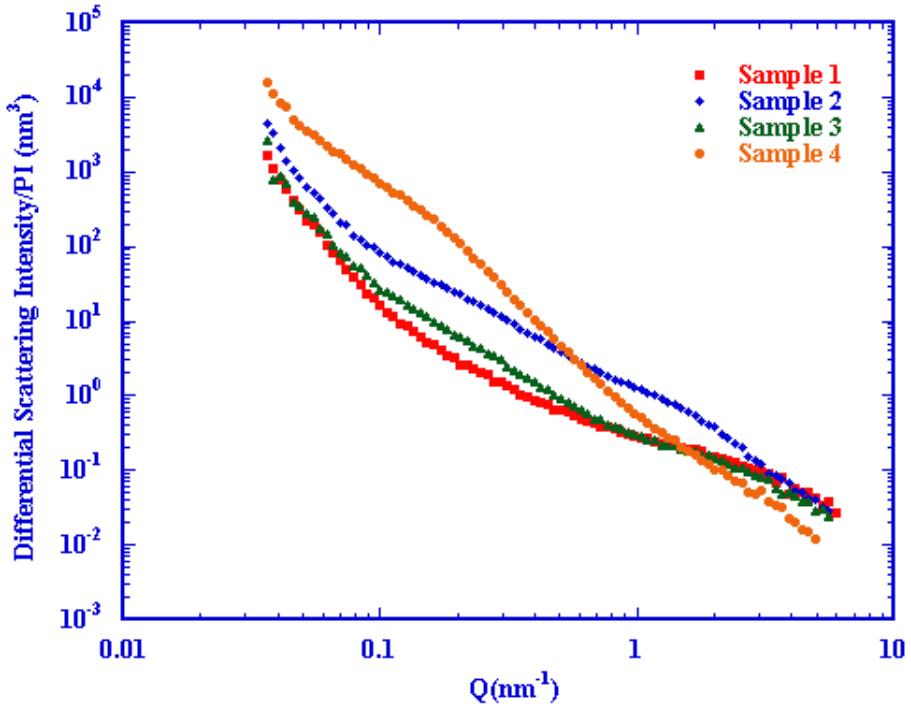

Figure 3. Differential scattering intensities (corrected by the Porod invariant) from the four "dry" activated carbon samples.

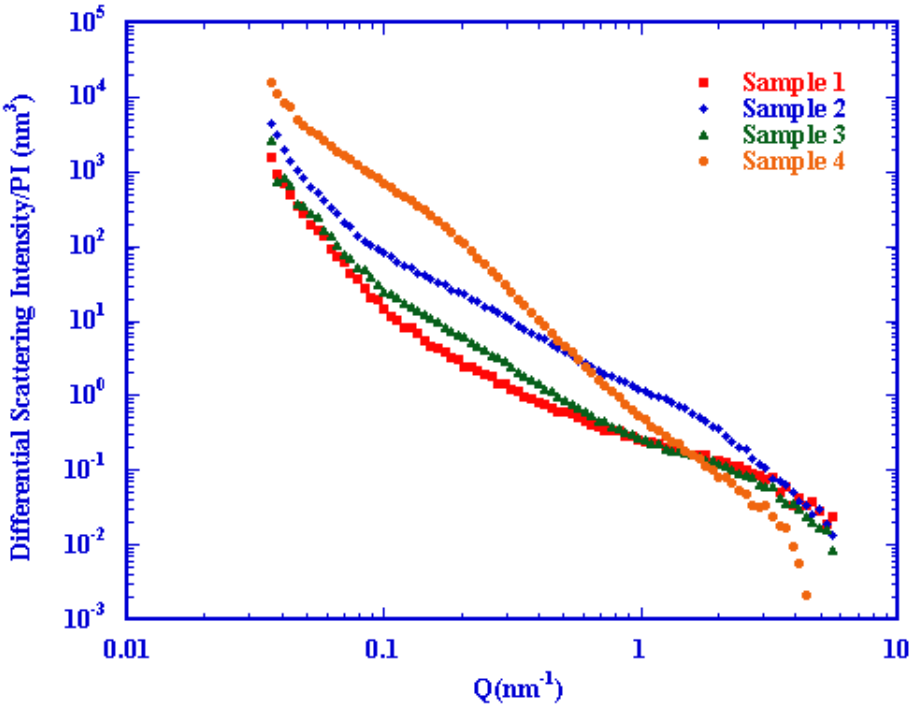

Figure 4. "Difference" differential scattering intensities determined from the "dry" and contrast-matched data (corrected by the Porod invariants) for the four carbon samples.

The fits to the integral pore volume distributions were differentiated to yield the differential pore size distributions presented in Figure 2 (for Sample 4, the data were differentiated directly for D > 4 nm). The results in Figure 2 are consistent with the descriptions of the samples presented above. The PSD for Sample 3 peaks *ca.* 1 nm, and exhibits the largest pore volume (except for Sample 4 for D > ~23 nm) and considerable mesoporosity. The PSD for Sample 1 exhibits the narrowest microporosity, also peaked at about 1 nm. Sample 4 exhibits the broadest PSD, with considerable much larger porosity, but lower total pore volume. Sample 2 also has a broad PSD, but with a larger pore volume.

In Figures 3 and 4 are presented the azimuthally-averaged, differential scattering intensities obtained for the four carbons, for both the "dry" samples (Figure 3), and the differences between the "dry" and contrast-matched samples (Figure 4). The scattering intensities were divided by the Porod invariant [13] of the "dry" and contrast-matched scattering curves in order to correct for the variation in the solid volume fraction, ϕ_s, with porosity [14]. In these data, the scattering contribution from the smaller scatterers (pores) are evident at high Q, and from the larger scatterers (pores) at low Q.

The contrast-matched scattering intensity data for all the carbons are not shown, since they were all similar and quite low, thereby indicating that the perdeuterated toluene effectively penetrated practically all the porosity; i.e., no "closed" porosity. The only exception to this behavior is the data for Sample 4 at high Q for the smallest pore sizes where the "difference" scattering intensity is significantly less than that for the "dry" samples. Consequently, the very smallest porosity for this sample is still "closed" to the exterior of the particle.

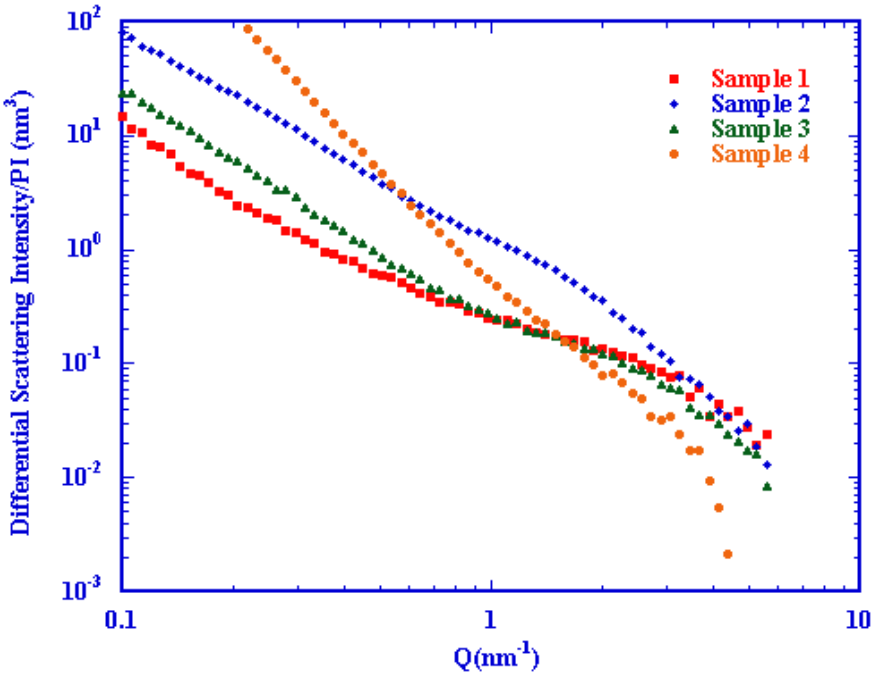

Figure 5. Enlargement of the "difference" differential scattering intensities from Figure 4 in the high Q range.

An enlargement of Figure 4 at high Q is presented in Figure 5. It shows that for the very smallest pores, the order of scattering intensities is Sample 1>2>3>4, although the PSDs of Samples 1 and 3 are very similar in this region. This is consistent with the derived PSD data in Figure 2. Sample 3 has a greater proportion of larger pores than Sample 1, and this too is consistent with the data in Figure 2. Sample 2 exhibits much greater scattering intensities than all the other samples over a very broad range for Q > 0.6 nm^{-1}, as is also apparent in its PSD in Figure 2. Scattering intensities for Sample 4 exceeded that of all the samples for Q < 0.6 nm^{-1}, and this too is apparent in the PSD data in Figures 1 and 2. It is noted that the effect of larger pores are amplified in the scattering data, due to the integral nature of the scattering intensity over all pore sizes raised to positive powers [14], whereas the opposite is true in differential representations of pore volume distributions, as in Figure 2.

Conclusions

A comparison of activated carbon porosity distributions from gas adsorption and SANS shows that the data from both techniques are consistent and complementary. In particular, SANS can be useful in determining the relative contribution of "closed" porosity, which is negligible for the well-activated carbons examined here, with the exception of the smallest porosity in Sample 4. In addition, SANS data is more sensitive to larger pore sizes. A combination of the two techniques can be used to provide a very complete representation of the porosity of activated carbons.

Acknowledgements

This work has benefited from the use of the Intense Pulsed Neutron Source at Argonne National Laboratory. This facility is funded by the U.S. Department of Energy, BES-Materials Science, under Contract W-31-109-Eng-38. The wood-based activated carbon samples were kindly provided by MeadWestvaco Corporation.

Table I - Surface Area and Pore Size Distribution of Activated Carbon Samples

Carbon Sample	BET Surface Area (m^2g^{-1})	Pore Size Distribution from Nitrogen Adsorption Isotherm Data Volume (ml/g) in Pore Widths (nm)									
		DFT Analysis								BJH Analysis	
		< 0.7	< 1.0	< 1.5	< 2	< 4	< 8	< 16	< 32	< 50	< 100
1	2500	0.11	0.45	0.69	0.90	1.09	1.11	1.12	1.12	1.14	1.14
2	1650	0.12	0.19	0.32	0.45	0.78	0.96	1.10	1.12	1.12	1.13
3	3230	0.10	0.30	0.61	0.91	1.45	1.57	1.62	1.64	not measured	
4	1690	0.09	0.26	0.41	0.51	0.66	0.76	1.07	2.29	not measured	

References

[1] Baker, F. S., Miller, C. E., Repik, A. J., and Tolles, E. D., Kirk-Othmer Encyclopedia of Chemical Technology, 4th Ed., Vol. 4, pp. 1015-1037; John Wiley & Sons, 1992.

[2] Wigmans, T., *Carbon*, **27**, pp. 13-22 (1989).

[3] Jagtoyen, M., and Derbyshire, F., *Carbon*, **36**, pp. 1085-1097 (1998).

[4] Baker, Frederick S., United States Patents 5,416,056 (May 16, 1995), 5,626,637 (May 6, 1997), 5,710,092 (Jan 20, 1998), and 5,965,483 (Oct 12, 1999), assigned to MeadWestvaco Corporation.

[5] Baker, F. S., "Development of a Highly Microporous Carbon for Natural Gas Storage," American Carbon Society Workshop on Gas Storage, Royal Military College of Canada, July 10-12, 2001.

[6] Lozano-Castello, D., Lillo-Rodenas, M. A., Cazorla-Amoros, D., and Linares-Solano, A., *Carbon*, **39**, pp. 741-749 (2001).

[7] Lillo-Rodenas, M. A., Lozano-Castello, D., Cazorla-Amoros, D., and Linares-Solano, A., *Carbon,* **39**, pp. 751-759 (2001).

[8] Lillo-Rodenas, M. A., Cazorla-Amoros, D., and Linares-Solano, A., *Carbon,* **41**, pp. 277-284 (2003).

[9] Brunauer, S., Emmett, P. H., and Teller, E., *J. Am. Chem. Soc*., **60**, pp. 309-319 (1938).

[10] Barrett, E. P., Joyner, L. G., and Halendar, P. H., *J. Am. Chem. Soc*., 73, 373 (1951).

[11] Lastoskie, C., Gubbins, K. E., and Quirke, N., J. Phys. Chem., 97, 4786 (1993).

[12] Jagiello, J., and Thommes, M., *Carbon,* 42, pp. 1227-1232 (2004).

[13] Higgins, J.S., and Benoît, H.C. Polymers and Neutron Scattering, Oxford University Press, 1994.

[14] Calo, J.M., Hall, P.J., Houtmann, S., Lozano-Castelló, D., Winans, R.E., and Seifert, S. ."Real time" determination of porosity development in carbons: a combined SAXS/TGA approach," in *Studies in Surface Science and Catalysis, Characterization of Porous Solids VI,* F. Rodríguez-Reinoso, B. McEnaney, J. Rouquerol, and K. Unger, eds., Elsevier, Amsterdam, 2002.